REMOVING ATMOSPHERIC EFFECTS FROM AVIRIS DATA FOR SURFACE REFLECTANCE RETRIEVALS

Bo-Cai Gao[1], Alexander F. H. Goetz[1,2], and J. A. Zamudio[1,2]

[1]Center for the Study of Earth from Space/CIRES, Campus Box 449,
[2]Department of Geological Sciences
University of Colorado, Boulder, CO

Abstract. Analysis of high resolution imaging spectrometer data requires a thorough compensation for atmospheric absorption and scattering. A method for retrieving surface reflectances from spectral data collected by the Airborne Visible/Infrared Imaging Spectrometer (AVIRIS) is being developed. In this method, the integrated water vapor amount on a pixel by pixel basis is derived from the 0.94- and 1.14-μm water vapor features. The water vapor, carbon dioxide (CO_2), oxygen (O_2) and methane (CH_4) transmission spectrum in the 0.4-2.5 μm region is calculated. The derived water vapor value and the solar and observational geometry are used in the spectral calculation. The AVIRIS spectrum is ratioed against the transmission spectrum to obtain the surface reflectance spectrum. Major mineral absorption features near 2.2 μm in retrieved reflectance spectra can be identified. Different vegetation absorption characteristics are observed. At present, the method is most useful for deriving surface reflectances from AVIRIS data measured on clear days with high visibilities. Atmospheric scattering effects will be included in our spectral calculations in the near future.

I. Introduction

Imaging spectrometers acquire images in hundreds of contiguous spectral bands such that for each picture element (pixel) a complete reflectance or emittance spectrum can be derived from the wavelength region covered (Goetz et al., 1985). In the coming decade, NASA expects to carry the High Resolution Imaging Spectrometer (HIRIS) (Goetz and Herring, 1989) aboard a platform of the Earth Observing System (Eos). The precursor to HIRIS is the Airborne Visible/Infrared Imaging Spectrometer (AVIRIS) (Vane, 1987), which is now operational. AVIRIS covers a spectral region from 0.4-2.5 μm in 10-nm bands and has a ground instantaneous field of view of 20x20 m from an altitude of 20 km. Because solar radiation is subject to atmospheric absorption and scattering in the combined Sun-surface-aircraft ray path, the radiance obtained by AVIRIS is modified by the atmosphere as well as by the Earth's surface materials. In order to properly infer the surface reflectances from AVIRIS data, accurate modeling of atmospheric absorption and scattering is necessary.

Figure 1 shows an AVIRIS spectrum measured over Rogers Dry Lake, California in February, 1990. The atmospheric water vapor absorption bands centered at approximately 0.94, 1.14, 1.38 and 1.88 μm, the oxygen bands at 0.96 and 1.27 μm, and the carbon dioxide band near 1.60 and 2.08 μm are clearly seen. Approximately half of the 0.4-2.5 μm region is affected by atmospheric gas absorptions. These atmospheric features, mainly those of water vapor, must be removed in order to obtain the surface reflectances.

II. Background

The radiance at a downward looking aircraft sensor can be written in a simplified form as

$$L_{Sensor}(\lambda) = L_{Sun}(\lambda)T(\lambda)R(\lambda) + L_{Path}(\lambda) \qquad (1)$$

where λ is the wavelength, $L_{Sensor}(\lambda)$ is the radiance at the sensor, $L_{Sun}(\lambda)$ is the solar radiance above the atmosphere, $T(\lambda)$ is the total atmospheric transmittance in the Sun-surface-sensor path, $R(\lambda)$ is the surface reflectance at the observational geometry, and $L_{Path}(\lambda)$ is the scattered path radiance, including effects of single scattering and multiple scattering. Near 0.5 μm, $L_{Path}(\lambda)$ resulting from Rayleigh and aerosol scattering is typically 50% or greater of the observed radiance. At wavelengths longer than 0.8 μm, the Rayleigh scattering effect is small, and $L_{Path}(\lambda)$ resulting mainly from aerosol scattering is on the order of 10% of the observed radiance. If the atmospheric transmittance is modeled and the path radiance is not modeled in the derivation of surface reflectances, errors of approximately 10% will be introduced in the derived surface reflectances beyond 0.8 μm.

A practical method, called the "empirical line method", for retrieving surface reflectances from AVIRIS data, has been developed by Conel et al. (1987). In this method, field measurements of surface reflectances of two targets having contrasting albedos are required. From Eq. (1), it is seen that $T(\lambda)$ and $L_{Path}(\lambda)$ can be derived from the AVIRIS radiance measurements over the two surface targets with known reflectances. The derived $T(\lambda)$ and $L_{Path}(\lambda)$ can then be used to obtain surface reflectances from AVIRIS data over other pixels, provided that $T(\lambda)$ and $L_{Path}(\lambda)$ remain constant within the image scene. The empirical line method also works well in retrieving surface reflectances from the raw AVIRIS data without radiometric calibration.

However, the empirical line method cannot effectively remove atmospheric gas absorption features from AVIRIS data over scenes with elevation variations. This is because atmospheric water vapor concentration usually decreases rapidly with height and transmittances within the scene vary with elevation. Figure 2 shows examples of derived surface reflectance curves from AVIRIS data measured over the Dolly Varden Mountains, Nevada in June, 1989 using the empirical line method. The strong water vapor absorption regions near 1.38 and 1.88 μm are not shown because these regions are opaque and contain no information from the surface. The top curve is an AVIRIS spectrum from an area lower in elevation than the two target areas used in the empirical line method, and the converse is true for the bottom curve. The top curve shows remaining water vapor features in the 0.94 and 1.14 μm regions, due to an under-correction of water vapor features with the empirical line method, while the bottom curve shows reversed water vapor features, due to an over-correction of water vapor features with the method. Figure 2 indicates that in order to remove water vapor features in AVIRIS data properly, water vapor values on a pixel-by-pixel basis are required. At present, the only practical way of obtaining the water vapor values on a pixel-by-pixel basis is to retrieve the values from the AVIRIS data themselves.

In this paper, a new method using atmospheric spectral simulations for deriving surface reflectances from AVIRIS data is described.

III. Method

The method for the derivation of surface reflectances from AVIRIS data consists of following steps:

1. The solar zenith angle is derived based on the AVIRIS' flight time and on the geographic location (latitude and longitude) of the scene.
2. Band positions and spectral resolution of AVIRIS data are verified by curve fitting absorption features of atmospheric water vapor, carbon dioxide, and oxygen. The spectral

calculation is made using a Malkmus narrow band model. The fitting is made using a nonlinear least squares program. Figure 3 shows an example of mismatching in band positions between an observed spectrum and a calculated spectrum. When this situation occurs, the band position of the observed spectrum is adjusted to obtain a better fit.

3. The AVIRIS radiance spectrum is divided by the solar radiance curve above the atmosphere (Iqbal, 1983). The resulting spectrum is referred to as the "apparent reflectance spectrum."

4. The integrated water vapor amount in the combined Sun-surface-sensor path on a pixel by pixel basis is derived from the 0.94- and the 1.14-μm water vapor features in the measured data using a band ratioing technique described in the Appendix.

5. The water vapor transmission spectrum in the 0.8-2.5 μm region is calculated using the Malkmus narrow band model and using the derived water vapor amount. The transmission spectra for well mixed gases, including carbon dioxide (CO_2), oxygen (O_2), and methane (CH_4), are calculated based on the solar and the observational geometry.

6. The apparent reflectance spectrum is then divided by the total atmospheric transmission spectrum in order to obtain the surface reflectance spectrum.

IV. Results

Our method for surface reflectance retrievals has been applied to several sets of AVIRIS data over different geographic locations. Figure 4 shows examples of derived reflectances of clouds, cloud shadow, and two types of vegetation, i.e., a golf course and pine trees, from AVIRIS data measured in June, 1989 over the Oregon Transact. It is interesting to note that the shapes of the two vegetation reflectance curves are different. The pine trees have lower reflectance near 1.7 μm region due to stronger lignin and cellulose absorptions. The golf course has lower reflectance in the 1.45-1.60 μm region due to stronger liquid water absorption.

Figure 5 shows examples of our derived surface reflectances from AVIRIS data gathered over the Dolly Varden Mountains, which contain different types of rocks. These spectra have been smoothed to 15 nm spectral resolution in order to allow better identification of broad mineral absorption features. For comparison, the reflectances obtained with the empirical line method from AVIRIS data over the same pixels, and the laboratory measured reflectances of rock samples collected from the field are also shown. A major carbonate feature near 2.34 μm is clearly seen in the upper three spectra. The lower three spectra are obtained from a quartz latite volcanic unit. The laboratory measured spectrum has nearly constant reflectances in the 2.0-2.4 μm region. The spectrum derived with our method has nearly constant reflectances in a smaller spectral region between 2.05 and 2.37 μm. The rapid drop off of our derived reflectance near 2.40 μm may be due to the fact that water vapor continuum absorption is not included in our spectral model. The above comparisons indicate that our method does a reasonably good job in recovering surface reflectance properties.

V. Discussion

The methane absorption near 2.35 μm is often considered unimportant in atmospheric modeling. For example, methane bands are not included in the 5S atmospheric transfer code (Tanre et al., 1990). However, we find that the peak absorption of the 2.35-μm methane band in a Sun-surface-sensor path is approximately 20%. It is necessary to include this methane band in the modeling. Otherwise, an error of the same magnitude will be introduced in the derived surface reflectances in the 2.35 μm region.

Our method for surface reflectance retrievals can only apply to AVIRIS data obtained on clear days with very low aerosol concentrations and for spectral regions above approximately 0.8 μm. Below 0.8 μm, atmospheric scattering must be modeled. Our method cannot be applied to AVIRIS spectra measured on hazy days, because under these situations significant portions of

measured radiation result from the aerosol scattering of solar radiation. Therefore, accurate modeling of atmospheric scattering effects is necessary.

When using our method for surface reflectance derivation, the band positions between observed and calculated spectra must be matched to 0.5 nm or better. Otherwise, peculiar features will appear in the derived surface reflectance curve, especially at the edges of atmospheric gaseous absorption features.

VI. Summary

A new method, using atmospheric spectral simulations for deriving surface reflectances from AVIRIS data, is described. The method is useful for surface reflectance retrievals in the 0.8-2.5 μm region from AVIRIS data measured on clear days with visibilities of 20 km or greater. The method has two advantages. One is that field measurements of surface reflectances are not required. The other is that atmospheric water vapor absorption features are removed on a pixel-by-pixel basis, based on the derived water vapor values from AVIRIS data themselves. Preliminary application of the technique to AVIRIS data indicates that retrieval results are reasonable. Different vegetation absorption characteristics are observed. Major mineral features are identified. In the near future, we plan to combine our program with the 5S code (Tanre et al., 1990) so that spectra corresponding to the AVIRIS' resolution and observational geometry can be calculated easily and that atmospheric scattering effects can be modeled approximately.

Acknowledgments

The authors are grateful to R. O. Green of the Jet Propulsion Laboratory for providing the AVIRIS spectral data. This work was partially supported by the Jet Propulsion Laboratory, California Institute of Technology under contract 958039 and the NASA Goddard Space Flight Center under a contract.

References

Conel, J. E., R. O. Green, G. Vane, C. J. Bruegge, and R. E. Alley, AIS-2 radiometry and a comparison of methods for recovery of ground reflectance, in *Proceedings of the Third Airborne Imaging Spectrometer Data Analysis Workshop, G. Vane, Ed., JPL Publ. 87-30*, 18-47, 1987.

Goetz, A. F. H., and M. Herring, The high resolution imaging spectrometer (HIRIS) for Eos, *IEEE Trans. Geosci. Remote Sens., 27*, 136–144, 1989.

Goetz, A. F. H., G. Vane, J. Solomon, and B. N. Rock, Imaging spectrometry for Earth remote sensing, *Science, 228*, 1147–1153, 1985.

Iqbal, M., *An Introduction to Solar Radiation*, pp. 43–95, Academic, San Diego, Calif., 1983.

Tanre, D., C. Deroo, P. Duhaut, M Herman, and J. J. Morcrette, Description of a computer code to simulate the satellite signal in the solar spectrum:the 5S code, *Int. J. Remote Sensing, 11*, 659-668, 1990.

Vane, G. (Ed.), Airborne visible/infrared imaging spectrometer (AVIRIS), *JPL Publ. 87–38*, Jet Propulsion Laboratory, Pasadena, Calif., 1987.

APPENDIX: BAND RATIOING METHOD

Figure A1 shows an apparent reflectance spectrum, in which the relevant positions and widths of spectral regions used in the band ratioing are illustrated. Specifically, apparent reflectances of 5 AVIRIS channels near 0.945 μm are averaged to give a mean apparent reflectance of the 0.94-μm water vapor band. Apparent reflectances of 3 channels near 0.86 μm are averaged to give a mean apparent reflectance at the 0.86 μm "atmospheric window" region. Apparent reflectances of 3 channels near 1.03 μm are averaged to obtain a mean apparent

reflectance at the 1.03 μm "atmospheric window" region. A mean observed transmittance for the 0.94-μm water vapor band is obtained by dividing the mean apparent reflectance at the water vapor center by one half of the sum of the mean apparent reflectances at the two window regions. A mean calculated transmittance for the 0.94-μm water vapor band is similarly obtained from a simulated spectrum with an assumed atmospheric temperature, pressure, and density model. A set of calculated mean transmittances for the 0.94-μm water vapor band is obtained from a set of simulated spectra with the same atmospheric model but with the amount of water vapor in the model being scaled by different factors. A table of water vapor amount as a function of calculated mean transmittance of the 0.94-μm water vapor band is obtained. The mean observed transmittance for the 0.94-μm water vapor band and a look-up table procedure are used to derive the amount of water vapor corresponding to the observed spectrum.

Similar band ratioing and look-up table procedures are used to derive water vapor amount from the 1.14-μm water vapor band. The average of water vapor values from the 0.94- and 1.14-μm bands is considered as the best estimate of the water vapor value corresponding to the spectrum.

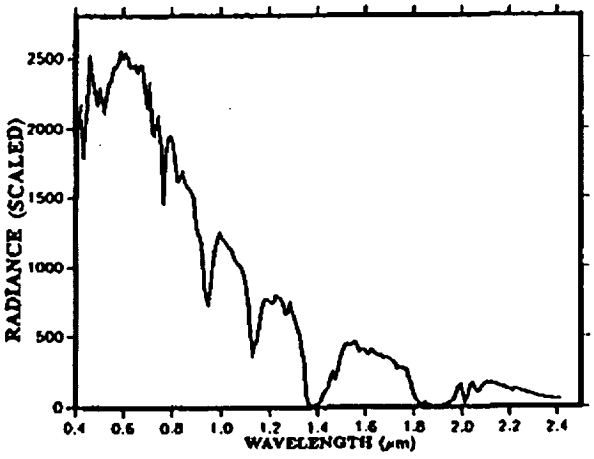

Fig. 1. An AVIRIS spectrum measured over Rogers Dry Lake, California in February, 1990. More than one third of the spectral region is affected by atmospheric water vapor absorption.

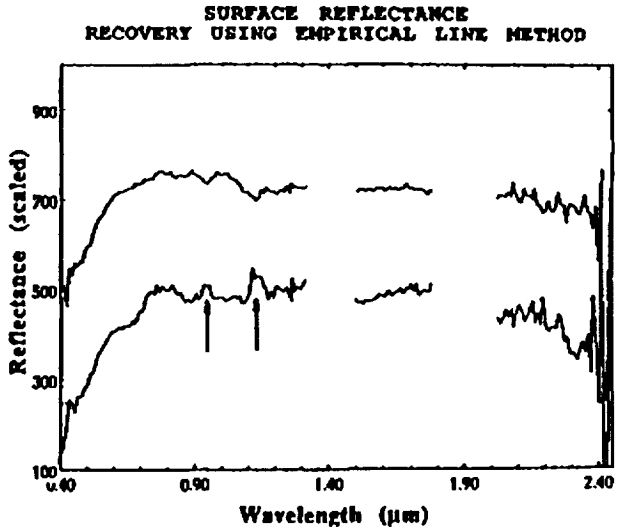

Fig. 2. Examples of derived surface reflectance spectra using the "empirical line method". Notice the under and over corrections of water vapor features near the 0.94 and 1.14 μm spectral regions.

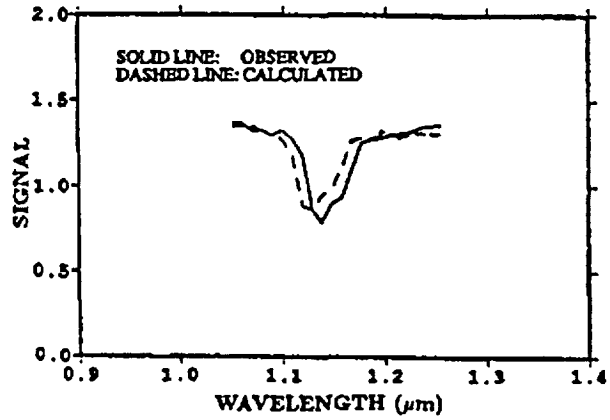

Fig. 3. An example of mismatch between calculated and observed spectra.

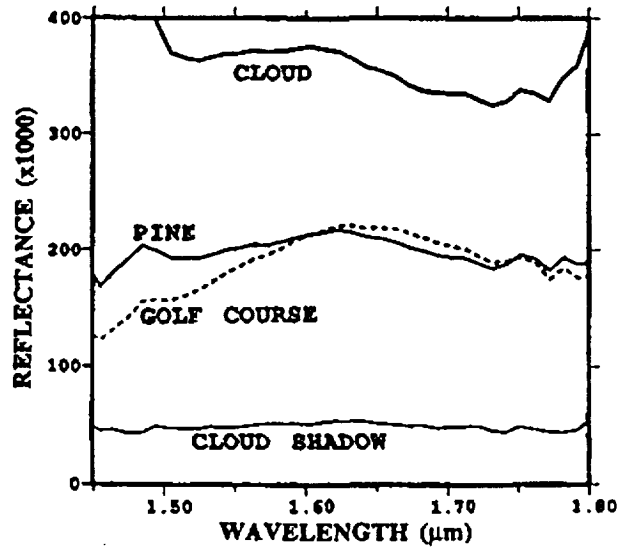

Fig. 4. Examples of derived reflectances of clouds, cloud shadows, and two types of vegetation from AVIRIS data measured in June, 1989 over the Oregon Transect.

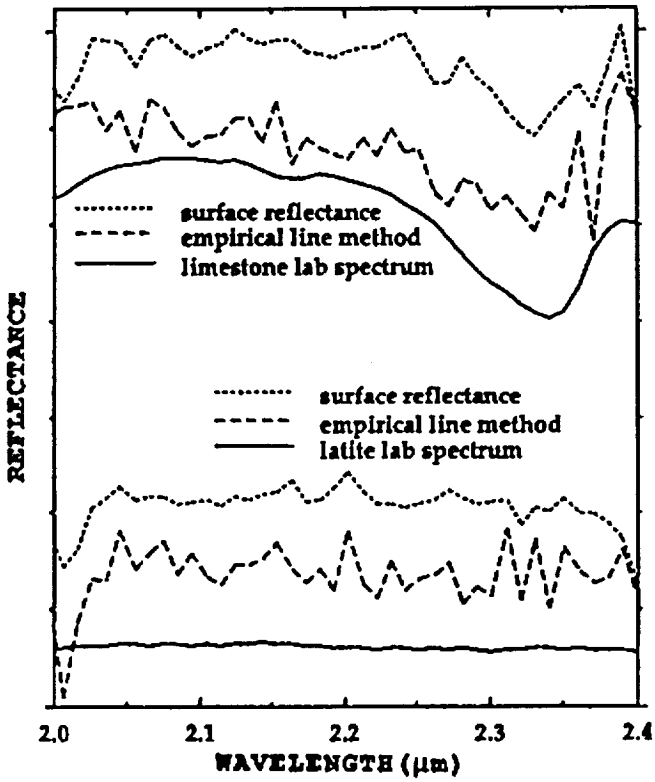

Fig. 5. Surface reflectance spectra obtained with three methods. See text for more descriptions.

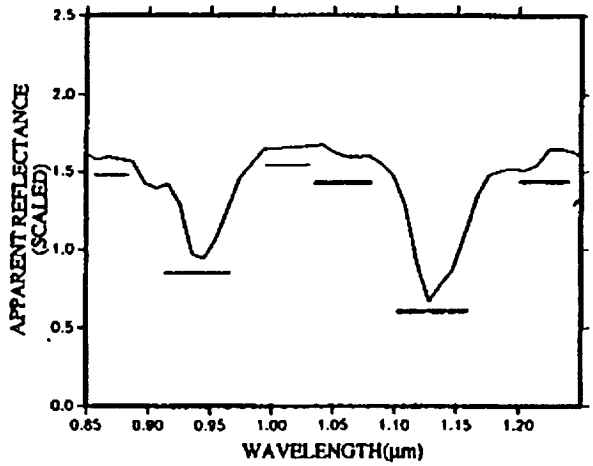

Fig. A1. An apparent reflectance spectrum with relevant positions and widths of spectral regions used in the band ratioing being illustrated.